Electron beam melting toward inclusion-free titanium alloys

H. Funagane[1]

[1] Advanced Technology Research Laboratories, Nippon Steel and Sumitomo Metal Corporation, 20-1 Shintomi, Futtu Chiba, 293-8511 Japan

Corresponding author : funagane.zq3.hitoshi@jp.nssmc.com

Abstract
Titanium ingots for airplanes must satisfy high standards of quality, removal of inclusions is essential. For the purpose of reducing the risk of contamination by LDI, a new way of removal of LDI has been studied. In the present study, marangoni flow induced by Intensive Heating of electron beam (IH) has been considered to control a state of a flow of molten metal in a cold crucible. Numerical simulations and an experiment have verified that LDI bounding for a lip was not able to go through the IH and stayed in a hearth.

Key words : Titanium, Electron beam melting, Removal of inclusions

1. Introduction

Titanium ingots or titanium alloys ingots for airplanes must satisfy high standards of quality, removal of inclusions is essential because they cause cracks in aero parts [1]. Since inclusions stay in raw material, removing them in the melt process is necessary. As one of the ways of melting raw material, electron beam melting with a cold crucible is used (see Fig.1) [2]. On the one hand, inclusions heavier than molten metal (called High Density Inclusions (HDI)) such as tungsten carbide sink in molten metal and stay in a hearth, so that the chance of contamination is almost zero. On the other hand, since inclusions like titanium nitrides and titanium oxides have porous structure, though their true densities are greater than molten metal, some of them move on the surface of molten metal and flow into a mold. This kind of inclusions is called Low Density Inclusions (LDI). Therefore, demands on reducing the risk of contamination by LDI are still high even these days [3, 4]. For the purpose of manufacturing inclusion-free ingots, a new way of removal of LDI has been studied.

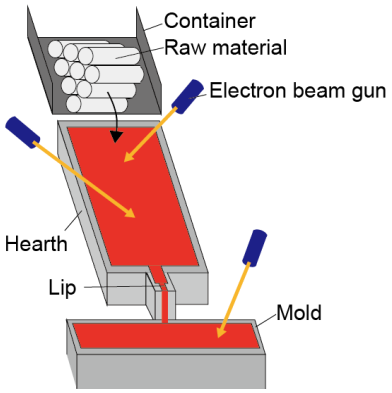

Fig. 1: An example of an electron beam furnace.

2. Methodology

It is well known that if there is a temperature gradient on the surface of fluid, Marangoni flow is induced. In the case of titanium, it flows from a high temperature place to a low temperature one. Thus, if some place of molten metal is intensively heated by electron beam (hereafter, we call Intensive Heating (IH)), marangoni flow originating there is induced because temperature of the heating place is higher than its surroundings. We thought that IH might be useful to control a state of a flow of molten metal in a cold crucible. More precisely, if molten metal in the crucible is heated without any reason except for keeping the temperature, since a uniform flow from the upstream side to the downstream side is formed, LDI moving on the surface of molten metal flow into a mold. But, if IH shown in Fig.2 is carried out, marangoni flow bounding for the upstream side from the IH zone is induced. As a result, LDI bounding for the mold stay in front of the IH zone (see Fig.3) and may be trapped or dissolved in the course of time.

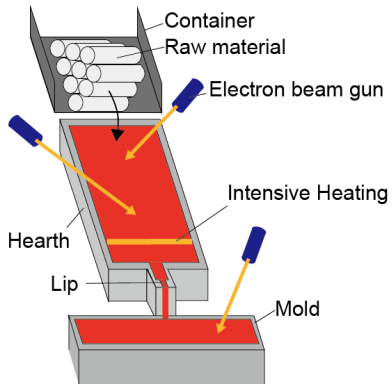

Fig. 2: An example of a beam path of Intensive Heating.

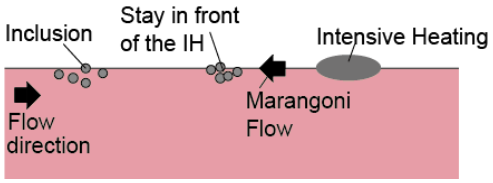

Fig. 3: Mechanism of removal of inclusions by Intensive Heating.

3. Numerical simulation

In order to verify whether Marangoni flow induced by IH can stop LDI moving on the surface of molten metal, a computational model describing a molten metal flow and an inclusion behavior in a cold crucible has developed [5-7] and numerical simulations have been carried out.

3.1. Computational model

Molten metal flow is described by the following equations:

$$\frac{\partial \rho}{\partial t} + \nabla \cdot (\rho \vec{v}) = 0 \tag{1}$$

$$\frac{\partial}{\partial t}(\rho \vec{v}) + \nabla \cdot (\rho \vec{v}\vec{v}) = -\nabla p + \nabla \cdot (\bar{\bar{\tau}}) + \rho \vec{g} - \rho \beta'(T - T_0)\vec{g} + \frac{(1-\beta)^2}{(\beta^3 + \varepsilon)} A_{mesh} \vec{v} \tag{2}$$

$$\bar{\bar{\tau}} = \mu[(\nabla \vec{v} + \nabla \vec{v}^T) - \frac{2}{3} \nabla \cdot \vec{v} I] \tag{3}$$

$$\frac{\partial}{\partial t}(\rho H) + \nabla \cdot (\rho \vec{v} H) = \nabla \cdot (k \nabla T) \tag{4}$$

$$H = c_P T + \beta L \tag{5}$$

$$\begin{cases} \beta = 0 & \text{if} \quad T < T_S \\ \beta = 1 & \text{if} \quad T > T_L \\ \beta = \dfrac{T - T_S}{T_L - T_S} & \text{if} \quad T_S < T < T_L \end{cases} \tag{6}$$

Here, t is time, ρ is density, $\vec{v}$ is velocity, p is pressure, $\bar{\bar{\tau}}$ is stress tensor, μ is viscosity, I is unit matrix, $\vec{g}$ is gravitational acceleration, β' is thermal expansion coefficient, T_0 is reference temperature, β is liquid fraction, $\varepsilon = 10^{-3}$, $A_{mesh} = 10^5$, k is thermal conductivity, T is temperature, c_P is specific heat, L is latent heat, T_S is solidus temperature, T_L is liquidus temperature.

Behavior of inclusion is written by the below equation:

$$\frac{d\vec{u}_P}{dt} = \frac{\vec{v} - \vec{u}_P}{\tau_r} + \frac{\vec{g}(\rho_P - \rho)}{\rho_P} \tag{7}$$

$$\tau_r = \frac{\rho_P d_P^2}{18\mu} \frac{24}{C_d Re} \tag{8}$$

$$Re = \frac{\rho d_P |\vec{u}_P - \vec{u}|}{\mu} \tag{9}$$

Here, the first term of the right hand side of Eq. (7) represents drag force. And, τ_r is relaxation time, $\vec{u}_P$ is particle velocity, ρ_P is particle density, d_P is particle diameter, C_d is drag force coefficient [8], Re is relative Reynolds number.

3.2. Numerical conditions and results

Behavior of LDI moving on the surface of molten metal has been investigated by the computational model under the following assumptions:

- Electron beam
  - ① Amount of heat: 0.25 MW
  - ② Scan velocity of an electron beam gun: 1.6 m/s
- LDI
  - ① Diameter: 5.0 mm
  - ② Density: -10 % lower than that of molten metal

A numerical result of behavior of LDI without IH is shown in Fig.4. In it, molten metal flows from the left hand side to the right hand side, so that the trajectory of LDI shown by a solid line is reaching to the right edge. This means that LDI can flow into a mold.

Numerical results of the case with IH are shown in Fig.5. In the figures of temperature, some place where temperature becomes highest is corresponding to a beam spot. In other words, in state 1, the beam spot is located at one of the edge of a beam path. In state 2, the spot is located at the center of the path. In state 3, the spot is located at other edge of the path. In the figures of behavior of LDI, the trajectories of LDI shown by a solid line stop at near the center of the hearth. That is, IH can stop LDI. In other words, IH can reduce the risk of contamination.

State	Surface temperature	Behavior of LDI
1		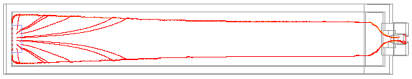
	300 K 2200 K	

Fig. 4: Behavior of LDI without Intensive Heating.

State	Surface temperature	Behavior of LDI
1	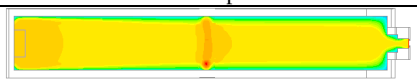	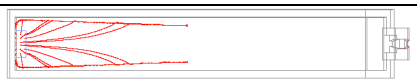
2	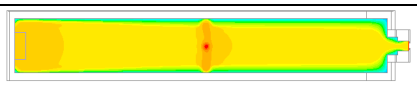	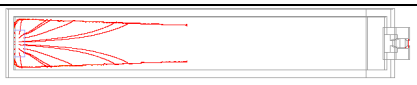
3	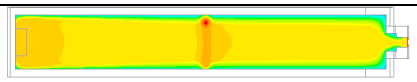	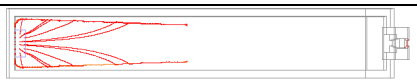
	300 K 2700 K	

Fig. 5: Behavior of LDI with Intensive Heating.

4. Experiment

In order to verify whether Marangoni flow induced by IH can stop LDI moving on the surface of molten metal even in an actual furnace, an experiment carried out. In it, a piece of graphite mixing into raw material was used as a tracer because the density was lower than that of titanium and the boiling point was more than 3000 ℃. Time transition of a piece of graphite without IH is shown in Fig. 6. The graphite moving on the surface of molten metal from the upstream side to the downstream side finally flowed into a mold. Meanwhile, that with IH is shown in Fig. 7. The graphite was stopped at IH zone and was not able to go through. That is, the effect of IH has been verified.

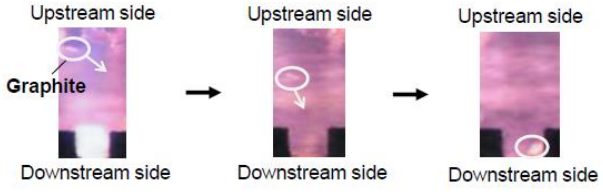

Fig. 6: Time transition of a piece of graphite without IH.

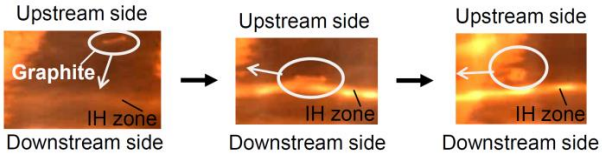

Fig. 7: Time transition of a piece of graphite with IH.

Acknowledgment
The authors appreciate all coworkers of this study for their support, encouragement and advices. Above all, help of Mr. Takeda and engineers at Naoetsu Works for the experiment was essential, so that we thank them enough.

References

1. A. Mitchell, ACTA METALLURGICA SINICA (ENGLISH LETTERS), 12 (1999), 283-296.
2. A. Mitchell, Materials Science and Engineering A, 263 (1999), 217-223.
3. J.P. Bellot, B. Foster, S. Hans, E. Hess, D. Ablitzer and A. Mitchell, Metallurgical and Materials Transactions B, 28B (1997), 1001-1010.
4. J.P. Bellot, E. Hess and D. Ablitzer, Metallurgical and Materials Transactions B, 31B (2000), 845-854.
5. J.P. Bellot, V. Descotes and A. Jardy, Numerical Modeling, 65 (2013), 1164-1172.
6. X. Zhao, Master's thesis of the University of British Columbia, (2006).
7. Z. Zhang, Master's thesis of the University of British Columbia, (2013).
8. S.A. Morsi and A.J. Alexandar, J. Fluid Mech., 55 (1972), 193-208.